Biological productivity and glaciomarine sedimentation in the Central Basin of the northwestern Ross Sea since the last glacial maximum

Boo-Keun Khim [a,*], Ester Colizza [b], Jae Il Lee [c], Federico Giglio [d], Sangbeom Ha [a], Young-Suk Bak [e]

[a] Department of Oceanography, Pusan National University, Busan, 46241, South Korea
[b] Department of Mathematics and Geosciences, University of Trieste, Trieste, Italy
[c] Division of Glacial Environment Research, Korea Polar Research Institute, Incheon, 24341, South Korea
[d] National Research Council-Institute of Polar Science, Bologna, Italy
[e] Earth Environmental System Research Center, Jeonbuk National University, Jeonju, 54896, South Korea

ARTICLE INFO

Keywords:
Glaciomarine
Geochemistry
Productivity
Ice sheet
Continental margin
Antarctica

ABSTRACT

This study documents multi-proxy data representing surface water productivity and AMS ^{14}C dates of box (BC3) and gravity (GC2) cores in the Central Basin of the northwestern Ross Sea. Based on AMS ^{14}C dates, a comparison of sediment properties between BC3 and GC2 reveals that BC3 records the complete Holocene (i.e., interglacial) history, which is correlated to the uppermost part of GC2. The lithostratigraphic succession of GC2 consists of the repetition of contrasting layers distinguished by the productivity proxies. In contrast to the uppermost sediment layer (i.e., interglacial), the subsurface sediment layer (i.e., deglacial) is distinctly characterized by very high biogenic components. Such pronounced biogenic remnants in the deglacial sediments are not explained exclusively by *in situ* enhanced productivity in the surface water. Our results, thus, suggest that eroded and reworked shelf sediments from a previous interglacial period enriched in biogenic components by the advancing ice sheet might be transported through the melt-water plumes from the grounding line to the Central Basin, to provide high geochemical properties of deglacial sediments. Thus, growth and retreat of the grounded ice sheet played an important role in glaciomarine sedimentation change in the Central Basin of the northwestern Ross Sea.

1. Introduction

The Antarctic polar system is characterized by interaction and interplay of oceanic, glaciological, atmospheric, and continental processes operated at multiple spatio-temporal scales (Colleoni et al., 2018). Despite such complicated environmental factors, the depositional model of glaciomarine sedimentation on the Antarctic continental shelf supports the biological productivity model proposed for the Weddell Sea continental margin by Grobe and Mackensen (1992). Based on the biological productivity model, more biogenic components are deposited on the seafloor of the continental margin during interglacial periods because of enhanced productivity under reduced sea ice cover, whereas fewer biogenic components are detected during glacial periods because of reduced productivity under more sea ice cover. Such a binary concept of biogenic sedimentation has also been applied successfully to the continental shelf of the Ross Sea (e.g., Frignani et al., 1998; Nishimura et al., 1998; Salvi et al., 2006).

The complex continental shelf morphology of the Ross Sea, characterized by a rugged topography with deep troughs and banks, has been shaped by the advance and retreat of the Ross Ice Sheet, preserving the signature of grounded and floating ice activity during the last glacial–interglacial cycle. The sedimentary stratigraphic sequence of the continental shelf (including shelf basins such as Drygalski Basin, JOIDES Basin, and Pennell Trough) in the Ross Sea has thus provided an unequivocal depositional model (Anderson et al., 1984; Domack and Harris, 1998; Anderson 1999; Domack et al., 1999). The typical sedimentary succession in the continental shelf of the Ross Sea shows an upward transition from subglacial or glaciomarine diamicton toward proximal to distal deglacial glaciomarine sediments, and late Holocene marine biogenic mud, recording a progressive retreat of the grounding line and the final onset of seasonal open marine conditions.

Much of the eroded debris excavated from the continental shelf by

* Corresponding author.
E-mail addresses: bkkhim@pusan.ac.kr (B.-K. Khim), colizzae@units.it (E. Colizza), leeji@kopri.re.kr (J.I. Lee), federico.giglio@cnr.it (F. Giglio), sb_ha@pusan.ac.kr (S. Ha), sydin@jbnu.ac.kr (Y.-S. Bak).

repeated ice sheet grounding during the deglacial and glacial periods was transported continuously toward the continental slope and rise, as well as the deep-sea abyssal plain in the Antarctic Ocean (Anderson, 1999). In contrast to the Antarctic continental shelf, the sedimentation in the Antarctic continental margin (particularly continental slope and rise) was more complex and difficult to explain by the simple stratigraphic succession. The continental slope sedimentation was more influenced by the dominant oceanographic processes along with bottom current activity, glacial meltwater plumes, and downslope sediment transport by sediment gravity flows (Anderson et al., 1984). Despite few detailed examinations of glaciomarine and hemipelagic sediments on the continental slope and rise of the Ross Sea, most of sediment cores exhibit considerable downcore variability characterized by massive and poorly-sorted glaciomarine sediments interbedded with laminated sediments that might be contourite or fine-grained turbidite (Anderson et al., 1979).

Based on the biological productivity model successfully applied to the stratigraphic successions in the Antarctic continental shelf, the present study revealed that the glaciomarine (interglacial-deglacial-glacial) sediments in the Central Basin, which is located in the continental slope of the northwestern Ross Sea, are not simply interpreted by the biological productivity model. Thus, our results suggest that the application of the biological productivity model to the Ross Sea continental slope requires more caution to complement the reliable paleoenvironmental reconstruction.

2. Material and methods

We collected a box core (BC3, 37 cm long) and a gravity core (GC2, 232 cm long) at site KI-13-C2 (71°52.5′S, 177°48.1′E, ~1800 m deep) located on a small terrace of Hallett Ridge in the Central Basin during the KOPRI ANA03B cruise onboard the IBRV *ARAON* in February 2013 (Fig. 1 and S1). The Central Basin forms a slope basin off the mouth of the JOIDES Basin in the northwestern Ross Sea. The sediment samples for the experimental analyses were taken at 1 cm interval for BC3 and at 2 cm intervals for GC2 at Trieste University (Italy). All analytical results are provided in the Supplemental material (Tables S1-S6).

Measurement of magnetic susceptibility (MS) was conducted using a Bartington magnetic susceptibility meter equipped with probe MS-2C magnetic susceptibility loop sensor (units in SI $\times 10^{-6}$) at 2 cm intervals at Italian National Research Council-Polar Science Institute of Bologna.

Prior to grain size analysis, the organic matter was eliminated using hydrogen peroxide and $CaCO_3$ was removed using a weak acetic acid, but the biogenic silica was not eliminated. The remaining sediments were sieved using a 2 mm mesh sieve net. Using a Malvern Mastersizer Laser Analyzer, the sediment particle sizes less than 2 mm at 1 cm interval for BC3 and at 8 cm intervals for GC2 were determined at University of Trieste. A S3500 laser diffraction particle analyzer (Microtrac) was also used to measure the grain size for the selected 6 samples of BC3 at Korea Institute of Geosciences and Mineral Resources (Korea). Sand (>63 μm), silt (63–2 μm), and clay (<2 μm) classes were decided using grain-size classification of Friedman and Sanders (1978). Grain size parameter was determined using the formulas of Folk and Ward (1957).

The biogenic silica content was analyzed by a wet alkaline extraction method modified from DeMaster (1981) at Pusan National University (Korea). The analytical error of biogenic silica content in sediment samples was less than 1%. Total inorganic carbon (TIC) content was measured using UIC CO_2 coulometer (Model CM5014) at Pusan National University. TIC content is converted to $CaCO_3$ content as weight percentage by the multiplication of factor 8.333. The analytical precision as relative standard deviation is 2%. Total carbon (TC) and total nitrogen (TN) contents were measured using an elemental analyzer (Model Flash 2000) at Pusan National University. The analytical precision as a relative standard deviation (±1σ) is 1%. Total organic carbon (TOC) content was calculated by determining the difference between TC and TIC. C/N ratio was calculated by TOC/TN.

Carbon isotopic composition ($\delta^{13}C_{OM}$) of carbonate-free sediments was measured using elemental analysis-isotope ratio mass spectrometry (EA-IRMS: Europa Scientific 20-20 mass spectrometer) at Iso-Analytical Ltd (UK). All isotopic compositions were expressed in the conventional δ notation and reported as parts per thousand (‰):

$$\delta^{13}C = [(^{13}C/^{12}C)_{sample} / (^{13}C/^{12}C)_{VPDB} - 1] \times 10^3$$

Precision for $\delta^{13}C_{SOM}$ was approximately ±0.08‰.

Accelerator Mass Spectroscopy (AMS) ^{14}C dating was carried out at 1 sample (1 acid insoluble organic carbon: AIOC) for BC3 and 7 samples (3 AIOC and 4 *N. pachyderma* tests) for GC2. AMS ^{14}C dates were performed at the Poznań Radiocarbon Laboratory of Adam Mickiewicz University (Poland) and at the Alfred-Wegener-Institut Helmholtz-Zentrum für Polar-und Meeresforschung (AWI, Germany). The AMS ^{14}C dating ages were reported in Melis et al. (2021) and are also provided in Table 1.

For the age determination of core-bottom by diatom chronology, the dry sediments (~2 g) were placed in a 500 ml beaker, adding 25 ml of 30% H_2O_2 and 25 ml of 10% HCl, which were heated to oxidize the organic material and dissolve the carbonates, and then allowed to stand for 24 h. After completion of the reaction, samples were washed three times with distilled water. The residue was transferred to a 60 ml bottle and diluted to 60 ml for analysis. Slides for diatom analysis were made using the random settling method of Scherer (1994). Specific biostratigraphic diatoms were observed mainly by using a Nikon E400 microscope.

3. Age estimate of cores BC3 and GC2 in the Central Basin

In general, the ages of AIOC in the Antarctic surface sediments typically ranges between 2,000 and 3,000 yrBP, with older ages (5,000 to 10,0000 yrBP) in slowly accumulating slope sediments (Domack et al., 1989; Andrews et al., 1999). In addition, AMS ^{14}C chronologies using AIOC from bulk sediments are often compromised by contamination from reworked ancient organic carbon derived from glacial erosion and/or from the reworking of unconsolidated sediments (e.g., Mezgec et al., 2017). Because of the different carbonate and organic carbon matrices, AMS ^{14}C dates on carbonate were directly calibrated and those on AIOC were corrected prior to the calibration. AMS ^{14}C dates on *N. pachyderma* tests were converted into calibrated ages using MARINE 13 calibration curve (Reimer et al., 2013), assuming constant marine radiocarbon reservoir age of 1.195 kyr by addition of regional marine offset (ΔR = 0.79 kyr) to standard marine reservoir age (405 years) from the global marine reservoir effect (MRE) (Hall et al., 2010). On the other hand, despite uncertainty and high variability (1,900 to 3,000 years) of regional reservoir correction (Domack, 1992), the downcore AIOC AMS ^{14}C dates were corrected by subtracting the AIOC age (i.e., 5,050 yrBP) of the well-preserved core-top sediments of BC3, which accounts for the regional MRE and the local dead carbon contamination offset (LCO), assuming that both MRE and LCO did not change (Hall et al., 2010). The LCO-corrected AMS ^{14}C dates performed on AIOC ages were converted into calibrated ages using MARINE 13 calibration curve (Reimer et al., 2013). Uncorrected and calibrated AMS ^{14}C ages are summarized in Table 1 and all the ages reported in this study represent the calibrated ages (cal. yrBP) unless otherwise specified.

The uncorrected AMS ^{14}C age for the core-top sample of BC3 dates 5,050 yrBP, which is typical in the Antarctic Ocean (Domack, 1992), because it contains regional MRE and LCO, as is 7,110 yrBP at the core-top of GC2 (Table 1). A comparison of geochemical properties between BC3 and GC2 reveals that a certain interval (~4 cm) seems to be missing from the core-top of GC2 (Fig. 2). Thus, a slightly older age at the core-top of GC2 may be expected. No reversal of a successive ages at the upper part of GC2 indicates that the sediment deposition was continuous without serious interruption. As a result, AMS ^{14}C ages and comparison between BC3 and GC2 indicate that BC3 records mostly the

Table 1
AMS ^{14}C ages of BC3 and GC2 in this study. The results were adopted from Melis et al. (2021).

Core	sample depth	carbon source	conventional ^{14}C age	error (±1σ)	LCO	LCO-corrected ^{14}C age	LCO-corrected calibrated ^{14}C age	Sedimentation rate (cm/kyr)	lab code
	(cm)		(yr BP)		(year)	(yr BP)	(yr BP)		
BC3	0–1	AIOC	5050	37					Poz-69634
GC2	0–1	AIOC	7110	40	3950	3160	1998		Poz-69635
GC2	14–15	AIOC	11,780	80	3950	7830	7535	2.5	Poz-69636
GC2	22–23	foram	15,710	143	–		17,669	0.8	AWI-4812.1.1
GC2	36–37	foram	16,230	100	–		18,262	23.3	Poz-75519
GC2	48–49	foram	17,080	90	–		19,179	13.1	Poz#2-75519
GC2	54–55	foram	17,930	166	–		20,188	5.9	AWI-4813.1.1
GC2	92–93	AIOC	29,900	450	3950	25,950	28,856	4.4	Poz-121684

Holocene (11.7–0 ka) during Marine Isotope Stage (MIS) 1 (14–0 ka) and a small portion of pre-Holocene (MIS 2) history in the lowermost part (Fig. 2). Similar to BC3, the upper part of GC2 characterized by low TOC and $CaCO_3$ contents records the Holocene. The age of the sediment layer underneath the Holocene interval of GC2 can be determined by AMS ^{14}C ages, which indicate MIS 2 at around 92 cm (Fig. 3). During MIS 2, the sediment layer is divided into two intervals: one is characterized by high TOC and $CaCO_3$ content containing foraminifera shells, whereas another is low TOC and $CaCO_3$ content (Fig. 3). The lower part of GC2 older than MIS 2 cannot be dated using AMS ^{14}C, but it seems likely to have been deposited during MIS 3 based on AMS ^{14}C ages (Fig. 3). In the lower part of GC2, the sediment layer is divided into a similar repeating pattern on the basis of multi-proxy profiles (Fig. 3).

Taviani et al. (1993) first reported an extensive cover of late Pleistocene carbonate on the northwestern Ross Sea continental shelf and suggested that these carbonates were glacial marine deposits. Quaia and Cespuglio (2000) also suggested that the calcareous sediment layer of a gravity core (ANTA91-8, Fig. 1) in the northwestern Ross Sea was of glacial origin (related to MIS 2) by showing the uncorrected AMS ^{14}C ages of 16.0–25.9 kyr BP. Similarly, Bonaccorsi and Melis (2001) reported an increase of planktonic foraminifera during the last glacial maximum (LGM) from a gravity core (ANTA95-89C, Fig. 1) in the Ross Sea continental margin. Recently, Bart et al. (2016) observed *in situ* benthic foraminifera even from the ice-proximal diamict sediments of grounding zone wedge in the Glomar Challenger Basin of the eastern Ross Sea continental shelf. All these previous studies, considering also the AMS ^{14}C ages from GC2, confirm that the high $CaCO_3$ layer below the Holocene sediments of GC2 corresponds to the latter part of MIS 2.

Southern Ocean diatom biostratigraphy provides the potential of age resolution and determination of paleoenvironmental conditions (Cody et al., 2008). Zielinski et al. (2002) proposed that *Rouxia leventerae* and *R. constricta* were deposited under the Southern Ocean cold-water conditions, which placed the last occurrence datum (LOD) between the latest part of MIS 6 (~0.14–0.13 Ma) and the early part of MIS 8 (~0.3–0.28 Ma), respectively. The diatom biostratigraphic marker, *R. leventerae*, was successfully used to constrain core chronology in Powell Basin (Bak et al., 2018). Unfortunately, *R. leventerae* was not observed in the middle to lower part of GC3 (Fig. S2). First occurrence datum (FOD: 1.66–1.73 Ma: Cody et al., 2008) of *F. obliquecostata* in GC2 may be unreliable for age constraint because a high amount of reworked diatom species (e.g., *Actinocyclus ingens, Proboscia barboi, Rouxia diploneides, Stephanopyxis turris, Thalassiosira inura, T. vulnifica*) with older

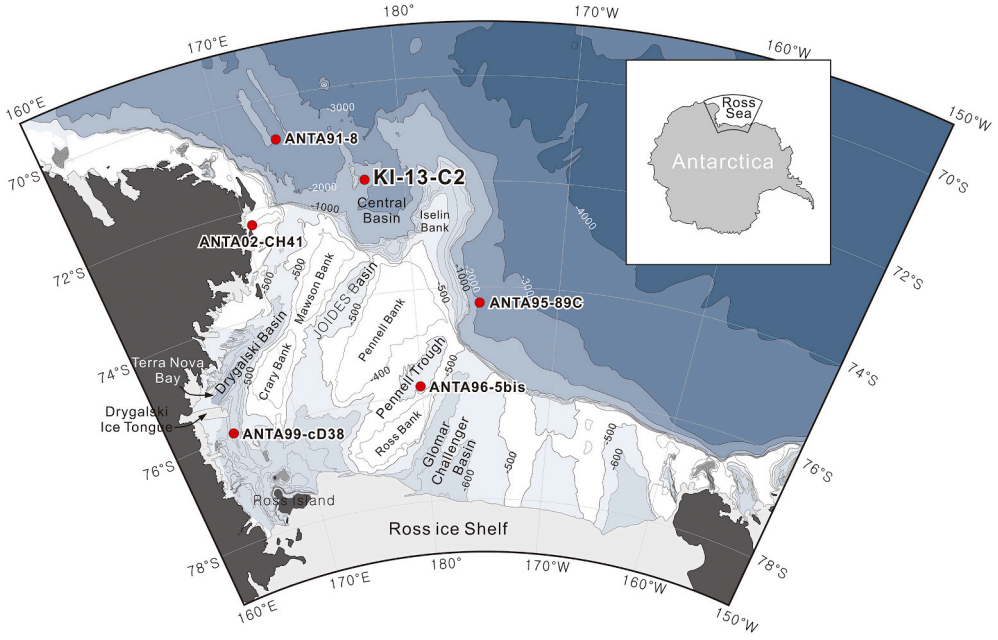

Fig. 1. Bathymetry of the Ross Sea showing the topographic features and the core location of this study (KI-13-C2) and other cores (ANTA91-8 from Ceccaroni et al., 1998, ANTA95-89C from Bonaccorsi and Melis, 2001, ANTA02-CH41 from Finocchiaro et al., 2005, ANTA99-cD38 from Finocchiaro et al., 2007, and ANTA96-5bis from Tolotti et al., 2013). Bathymetry data are taken from Davey (2004).

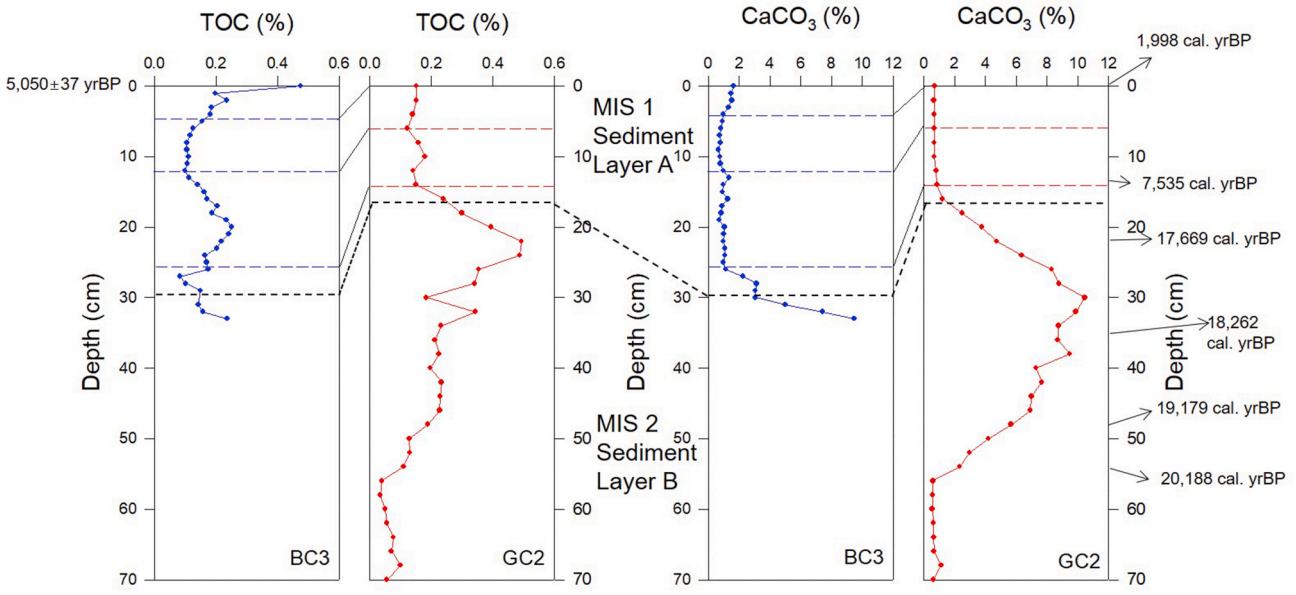

Fig. 2. Comparison of TOC and $CaCO_3$ between BC3 and GC2 for the examination of core-top preservation of GC2. A slight part of core-top of GC2 was lost during the coring operation. AMS ^{14}C ages of core-top of both cores validate the loss of core-top of GC2. A slight different thickness of same interval between two cores is due to the different pressure operation between the box corer and gravity corer. Core-top AMS ^{14}C age of BC3 is uncorrected and uncalibrated, whereas AMS ^{14}C ages of GC2 are LCO-corrected calibrated.

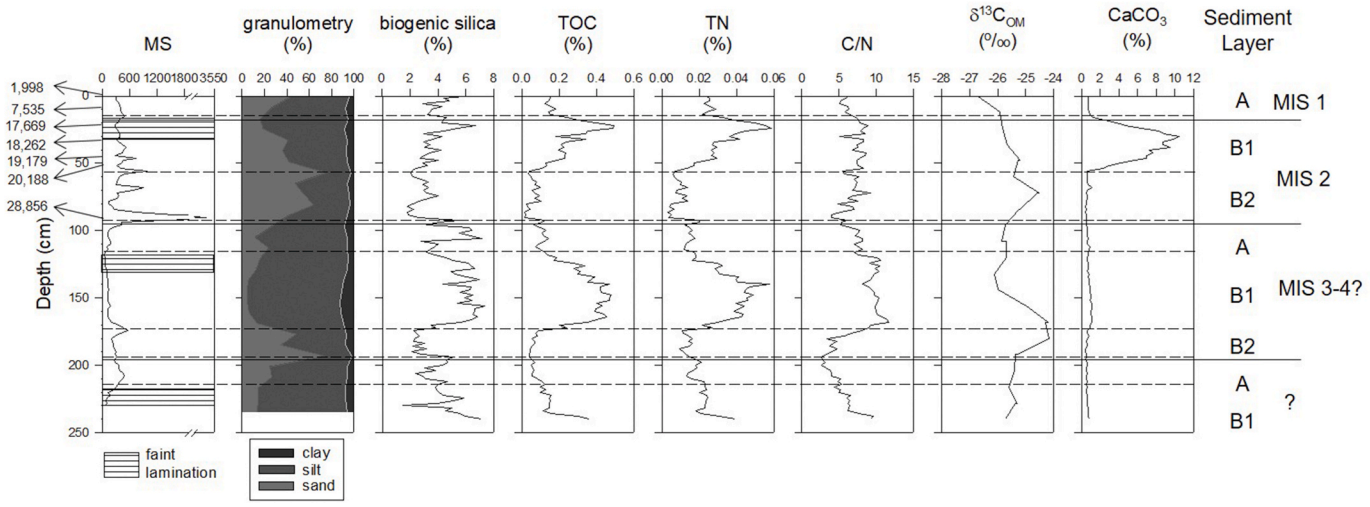

Fig. 3. Downcore profiles of the multi-proxy data (magnetic susceptibility: MS, sand-silt-clay content, biogenic silica, total organic carbon: TOC, total nitrogen, TN, C/N ratio, $\delta^{13}C_{OM}$, $CaCO_3$) of GC2. AMS ^{14}C ages of GC2 are noted in Table 1. The boundary of sediment layers (A, B1, B2) is not conclusive and a little arbitrary.

ages were present throughout the core. The expected core-bottom age by FOD of *F. obliquecostata* is much older than the age extrapolated by the sedimentation rate calculated by AMS ^{14}C dates. Thus, the precise age decision of core-bottom requires more additional approaches.

4. Results

The sediment interval of BC3 is characterized by parallel variation patterns of geochemical properties and upward fining trend (Fig. 4). Variation patterns of MS and sand fraction seem similar, except for the uppermost part. Geochemical properties (biogenic silica, TOC, and TN) are mostly consistent within a small range throughout the core, except for the sharp increase of TOC and TN at the core-top. One peculiar highlight is the core-top record (~7% of biogenic silica, ~0.5% of TOC, ~0.08% of TN, ~6 of C/N ratio, ~-27‰ of $\delta^{13}C_{OM}$ value, and <2% of $CaCO_3$) of BC3, which may represent the present-day conditions in the continental slope of the Ross Sea. Except for the lowermost part of high $CaCO_3$ content, BC3 represents the Holocene sediment layer.

Similar to BC3, the quantity of coarse-grained particles (i.e., ice-rafted debris: IRD) in GC2 is clearly related to the MS (Fig. 4). Low MS layers of fine-grained sediments are characterized partly by faint lamination (Fig. S3). The multi-proxy downcore profiles of GC2 specifically shows the repeated fluctuations of geochemical properties such as biogenic silica, TOC, TN, and C/N ratio (Fig. 4). The upper part (0–17 cm) of GC2, which corresponds to the Holocene sediments of BC3 (Fig. 2), is characterized by quite low values of these geochemical properties. This interval is defined as sediment layer A, which belongs to MIS 1. MIS 2 is divided into the two sediment layers (B1 and B2). Sediment layer B1 is characterized by high values of geochemical properties that may be associated with biological productivity (biogenic silica: ~7.1%, TOC: ~0.5%, TN: ~0.06%, and $CaCO_3$: ~11%), whereas values of these properties in sediment layer B2 are relatively low. The

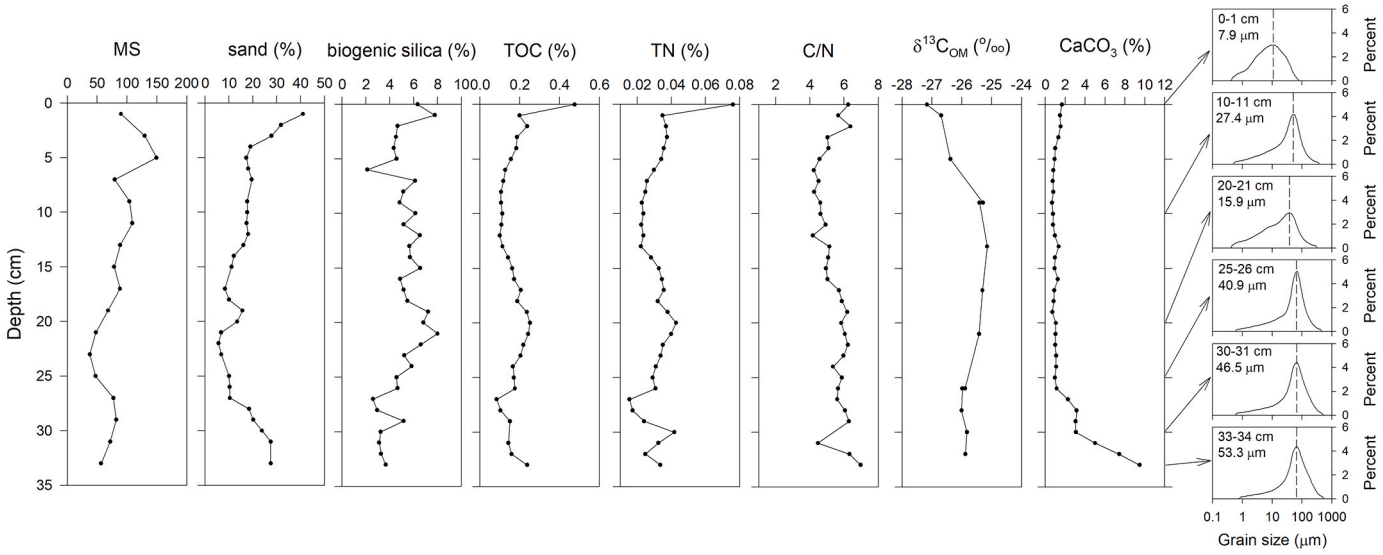

Fig. 4. Downcore profiles of the multi-proxy data (magnetic susceptibility: MS, sand content, biogenic silica, total organic carbon: TOC, total nitrogen: TN, C/N ratio, $\delta^{13}C_{OM}$, $CaCO_3$) of BC3. Six grain size distributions at the right were obtained from the bulk sediments.

succession of similar sediment layers is repeated in the lower part of GC2, although $CaCO_3$ content is quite low in the earlier B1 type layers (Fig. 3). The sediment layers of high biogenic silica, TOC, and TN contents are also characterized by faint fine-grained lamination. Thus, the stratigraphic succession of sediment lithology of GC2 shows the quasi-periodic changes in the sediment properties. These sediment layers may correspond to interglacial (sediment layer A), deglacial (sediment layer B1), and glacial (sediment layer B2) sequences chronologically (Fig. 3).

5. Discussion

No diamicton was clearly observed in GC2 in the Central Basin (Fig. 4), which is different from the typical depositional model of the continental shelf in the Ross Sea (Anderson et al., 1984; Domack and Harris, 1998; Anderson 1999, Domack et al., 1999). Content of coarse-grained particles governs the MS of sediment layers B1 and B2 (Fig. 3). This indicates that IRD was deposited on the continental slope by the fallout of coarse-grained detritus transported by icebergs during

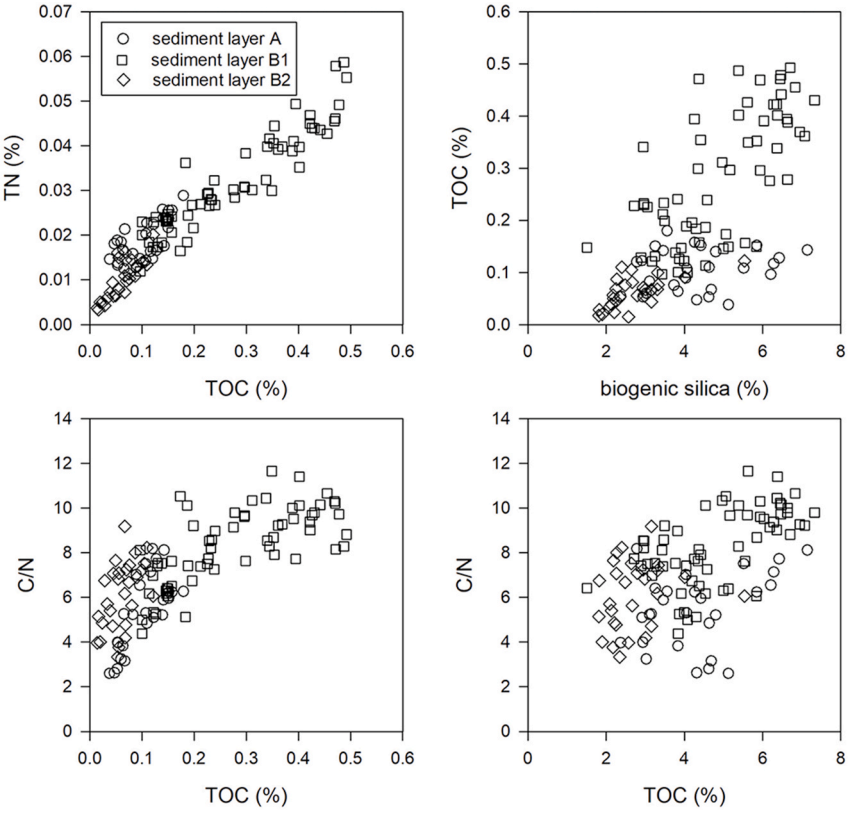

Fig. 5. Biplots of geochemical properties (TOC, TN, biogenic silica, C/N ratio) among the sediment layers A (interglacial), B1 (deglacial), and B2 (glacial) in GC2. The biogenic components of deglacial sediments are distinctly higher than those of the other sediments.

the deglacial and glacial periods (Anderson, 1999; Domack et al., 1999). The MS variation showing the intermittent MS peaks is not related to the sediment geochemical properties (Fig. 3). In contrast, it is worth noting that the faintly-laminated layers with very low coarse-grained particles (i.e., low MS) within sediment layer B1 are characterized by high biogenic silica (~7.1%), TOC (~0.5%), and TN (~0.06%) contents (Fig. 3). Sediment layer B2 is also characterized by the low values of these geochemical properties (Fig. 3). This remarkable contrast of biogenic components among sediment layers A, B1, and B2 is further highlighted in Fig. 5, exemplifying that the deglacial sediments are characterized by high biogenic components. The strong linear relationship between TOC and TN confirms that the organic matter in these sediment layers are of biogenic origin (Fig. 5). These bi-plots clearly separate the deglacial sediments from interglacial and glacial sediments. In particular, high TOC contents are correlated strongly to high biogenic silica contents, which may be attributed to the high biogenic productivity. However, high TOC contents are also characterized by high C/N ratios, which reflects that the sediment organic matter was not of marine origin and supports that sediment organic matters are reworked, not freshly-generated. Thus, our results suggest that the high biogenic components of deglacial sediments are not totally provided by *in situ* surface water production.

The Ross Sea continental shelf including its polynyas is a biological 'hot spot' of increased productivity marked by the highest phytoplankton concentration (10–40 mg Chl *a* m^{-3}) in the Southern Ocean (e.g., Arrigo et al., 2000). The biogenic silica production in the water column is a primary factor used to determine present-day patterns of biosiliceous sediment accumulation on the continental shelf of the Ross Sea, with the southwestern area being the most productive (~41% of biogenic silica; Ledford-Hoffman et al., 1986). According to Frignani et al. (1998), the present-day sedimentation on the continental shelf of the Ross Sea is dominated by biosiliceous mud and ooze ranging from 0.5 to 32.7% (13.5% on average) of biogenic silica and from 0.2 to 2.8% (0.88% on average) of TOC. The Holocene interval of BC3 and GC2, consisting of diatomaceous sandy mud, in the Central Basin indicates seasonally open marine conditions. As observed from the core-top record (~7% of biogenic silica, ~0.5% of TOC, and ~0.08% of TN) of BC3 (Fig. 3), the present-day biogenic content in the continental slope is quite low, compared to that of the continental shelf. Such difference in productivity level was corroborated by the decrease of chlorophyll concentration away from the coastal area to the deep marine environment (Arrigo et al., 2000).

Productivity proxies such as biogenic silica, TOC, and TN represent the surface water conditions; high productivity generally indicates a relatively warm and open marine environment, despite variations in preservation due to dissolution or degradation (Ledford-Hoffman et al., 1986; Arrigo et al., 2000). Thus, it is widely accepted that an interval of increased productivity defines the interglacial period in the Antarctic continental margin (e.g., Bonn et al., 1998). The sedimentary deposits on the continental shelf of the Ross Sea exhibit typical coupling between the sediment lithology and productivity changes: low productivity for glacial diamicton and high productivity for open marine Holocene mud with a transition from low to high during the deglacial condition (Frignani et al., 1998; Nishimura et al., 1998; Salvi et al., 2006). However, the application of such a straightforward biological productivity model to the lithologic succession of GC2 would lead to a misguided interpretation of enhanced productivity during the deglacial periods.

The increase in late Holocene biological productivity is clearly indicated by the biogenic silica, TOC, and TN of BC3 (Fig. 4). In contrast, such increase of productivity corresponds to a decrease in $\delta^{13}C_{OM}$ values, suggesting that $\delta^{13}C_{OM}$ values were not affected directly by dissolved inorganic carbon, but rather by the phytoplankton species diversity, physiological metabolism, or other factors (Rau et al., 1991). As $\delta^{13}C_{OM}$ values are determined by a combination of several factors (Popp et al., 1999), GC2 also shows that the variation patterns of $\delta^{13}C_{OM}$ are not closely related to the productivity proxies (Fig. 3), signifying that the deglacial maximum of biogenic silica, TOC, and TN was not likely supported by *in situ* enhanced surface water productivity. Hence, this abnormal elevation of the multi-proxy dataset during deglacial periods may be attributed to an alternative process, ruling out the simple surface water productivity change.

The deglacial interval (i.e., sediment layer B1) of GC2 characterized by the high productivity proxy consists of faintly laminated fine-grained sediments with rare IRDs and low MS (Fig. 3). Biogenic silica-rich lamination of the Antarctic deglacial sediments generally records the different seasonal fall-out distinguished by the diatom species and detrital particles (e.g., Alley et al., 2018). Early Holocene fine-grained laminated sediments (ANTA02-CH41, Fig. 1) from Cape Hallett Bay and pre-LGM laminated sediments (ANTA99-cD38, Fig. 1) from Nordenskjöld Basin, both of which are characterized by high biogenic silica and TOC, were interpreted as representing the increase of productivity under open marine conditions (Finocchiaro et al., 2005, 2007). Tolotti et al. (2013) also proposed a pre-LGM open marine condition in the Glomar Challenger Basin (ANTA96-5bis, Fig. 1) of the Ross Sea, although this sediment interval contains a high amount of reworked diatom taxa with older ages, as the robust reworked valves were dominant in the diamicton in the central Ross Sea (Sjunneskog and Scherer, 2005). On the contrary, Anderson et al. (1979) proposed that the laminated sediments on the Ross Sea continental margin were attributed to turbidites or contourites. Sprenk et al. (2014) suggested that fine-grained siliciclastic laminated sediments formed glacial contourite in the southeastern Weddell Sea by enhanced thermohaline convection in front of a grounded ice sheet. Thus, the faint lamination in the deglacial interval of GC2 should be carefully interpreted, raising the possibility that the laminated fine-grained sediments might have been deposited by different glaciomarine sedimentation events.

Based on glaciomarine sedimentation, the depositional model of the Ross Sea continental shelf contains glacial overconsolidated diamicton (e.g., Anderson, 1999; Domack et al., 1999). The absence of diamicton in GC2 represents that the depositional model of the continental slope differs from that of the continental shelf. In addition, GC2 clearly exhibits the repetition of contrasting layers: low biogenic content layer (sediment layer A) of the interglacial period, high biogenic content layer (sediment layer B1) of the deglacial period, and low biogenic content layer (sediment layer B2) of glacial period. Glaciomarine sedimentation of the interglacial layer in GC2 is similar to that operated in the continental shelf setting (Frignani et al., 1998; Nishimura et al., 1998; Salvi et al., 2006). Diatom-rich mud resulting from enhanced productivity under warm and open marine conditions accumulated under the influence of iceberg and sea-ice rafting near the calving front of the receding Ross Ice Shelf. As reported in the previous studies on continental shelf (Sjunneskog and Scherer, 2005; Tolotti et al., 2013), the diatoms of the interglacial sediments of GC2 are dominated by *Fragilariopsis curta* and *F. kerguelensis*, indicating winter sea ice and summer open marine conditions (Melis et al., 2021).

Lithologic contrast between the massive and laminated sediments on the Antarctic continental rise has been interpreted to differentiate different climate conditions (e.g., Damiani et al., 2006). For example, Khim et al. (2017) also differentiated two types of late Neogene marine sediments in the Wilkes land continental rise based on biogenic components as well as clay mineral compositions, which depend on the growth and retreat of the East Antarctic Ice Sheet and associated changes in sea ice. We suggested that the grounded ice sheet that led to the subglacial or glaciomarine diamicton on the continental shelf of the Ross Sea also plays a principal role in governing glaciomarine sedimentation in the Central Basin during the deglacial period. As explained, the biogenic productivity in the Central Basin during the glacial period was reduced due to the extensive sea ice coverage. Thus, deglacial fine-grained sediments characterized by high productivity proxies forming faint laminations in GC2 in the Central Basin might be deposited through the distal transport by melt-water plumes discharged from more extensive ice sheet that eroded and reworked shelf sediments containing

high contents of biogenic components and old mixed diatom species. Ha et al. (2019) also reported that the deglacial-glacial sediment layers of GC2 are characterized by more illite and chlorite content and less smectite content, which supports our interpretation of sediment deposition in the Central Basin. Finally, this deglacial deposit characterized by the high biogenic components in the Central Basin may also be used to establish the chronostratigraphic succession, despite the difficulty of limited dating on the Antarctic continental margin.

6. Conclusions

The advance and retreat of ice sheets leaves a uniform sedimentary signature on the continental shelf of the Ross Sea, applying the typical and uncomplicated depositional model (glacial overconsolidated diamicton overlain by deglacial glaciomarine sediments with an increase of IRD, which is in turn overlain by the late Holocene open marine biogenic mud). A comparison of multi-proxy data between BC3 and GC2, referenced to AMS ^{14}C dates, confirms that BC3 records a temporal lithologic succession from the late glacial period to the Holocene. Below the Holocene layer, the high $CaCO_3$ sediments mark the deglacial period, based on AMS ^{14}C dates. Compared to BC3, the sedimentary deposits of GC2 are divided into the repetition of three sediment layers (A, B1, B2), distinguished distinctly by the productivity proxy, corresponding to the interglacial-deglacial-glacial sequences. In particular, the deglacial sediments are characterized by higher biogenic content and faint lamination. The glaciomarine sedimentation caused by the melt-water plumes discharged from more extensive ice sheet, which probably eroded and reworked shelf sediments, resulted in an increase in biogenic remnants in the continental slope during the deglacial periods. The grounded ice sheet activity plays an important role in the glaciomarine sedimentation of the Ross Sea continental margin, leading to an abnormal record of high biological productivity in the deglacial sedimentary deposit. Hence, the repetition of the biogenic-rich deglacial deposit in the Central Basin does not simply result from local biological productivity. Thus, our results confirm that application of the biological productivity model should be integrated with understanding of the glaciomarine sedimentation regime.

Declaration of competing interest

The authors declare that they have no known competing financial interests or personal relationships that could have appeared to influence the work reported in this paper.

Acknowledgements

The captain, crew, and all onboard technicians (particularly, Mr. H.S. Moon) and researchers of IB Araon cruise in 2013 are thanked for core sampling. We appreciate Prof. John Anderson (Rice University) and Prof. Y.K. Sohn (Gyeongsang National University) on their fruitful comments on the depositional concept of the glaciomarine sedimentation in the continental slope of the northwestern Ross Sea. We also thank two anonymous reviewers and associate editor for their constructive comments to improve the manuscript. This study was carried out by the National Research Foundation of Korea (2019K1A3A1A25000116and 2019R1A2C1007701), partly by KOPRI project (PE21090), and by the Italian National Antarctic Research Program (PNRA) – ROSSLOPE Project (2010/A2.07) and partly co-funded by the Italian Foreign Ministry (MAECI) – STREAM Project.

References

Alley, K., Patacca, K., Pike, J., Dunbar, R., Leventer, A., 2018. Iceberg Alley, East Antarctic margin: continuously laminated diatomaceous sediments form the late Holocene. Mar. Micropaleontol. 140, 56–68.
Anderson, J.B., 1999. Antarctic Marine Geology. Cambridge University Press, Cambridge (UK), p. 289.
Anderson, J.B., Brake, C.F., Myers, N.C., 1984. Sedimentation on the Ross Sea continental shelf, Antarctica. Mar. Geol. 57, 295–333.
Anderson, J.B., Kurtz, D.D., Weaver, F.M., 1979. Sedimentation on the Antarctic continental slope. In: Pilkey, O., Doyle, L. (Eds.), Geology of Continental Slopes. Soc. Econ. Paleontol. Mineral. Sp. Pap. No. 27, pp. 265–283.
Andrews, J.T., Domack, E.W., Cunningham, W.L., Leventer, A., Licht, K.J., Jull, A.J.T., DeMaster, D.J., Jennings, A.E., 1999. Problems and possible solutions concerning radiocarbon dating of surface marine sediments, Ross Sea, Antarctica. Quat. Res. 52, 206–216.
Arrigo, K.R., DiTullio, G.R., Dunbar, R.B., Robinson, D.H., Van Woert, M., Worthen, D.L., Lizotte, M.P., 2000. Phytoplankton taxonomic variability in nutrient utilization and primary production in the Ross Sea. J. Geophys. Res. (Oceans) 105, 8827–8846.
Bak, Y.S., Yoo, K.C., Lee, J.I., Yoon, H.I., 2018. Glacial-interglacial records from sediments in Powell Basin, Antarctica. Antarct. Sci. 30, 371–378.
Bart, P.J., Coquereau, L., Warny, S., Majewski, W., 2016. In situ foraminifera in grounding zone diamict: a working hypothesis. Antarct. Sci. 28, 313–321.
Bonaccorsi, R., Melis, R., 2001. Persistence of living planktonic foraminifera (*Neogloboquadrina pachyderma*) in Antarctic sea-ice inferred from a study of a sediment core (Ross Sea continental margin). In: Chela-Flores, J., Owen, J., Raulin, F. (Eds.), First Steps in the Origin of Life in the Universe. Kluwer Academic Publishers, Netherlands, pp. 255–260.
Bonn, W.J., Gingele, F.X., Grobe, H., Mackensen, A., Futterer, D.K., 1998. Palaeoproductivity at the Antarctic continental margin: opal and barium records for the last 400 ka. Palaeogeogr. Palaeoclimatol. Palaeoecol. 129, 195–211.
Ceccaroni, L., Frank, M., Frignani, M., Langone, L., Ravaioli, M., Mangini, A., 1998. Late Quaternary fluctuations of biogenic component fluxes on the continental slope of the Ross Sea, Antarctica. J. Mar. Syst. 17, 515–525.
Cody, R.D., Levy, R.H., Harwood, D.M., Sadler, P.M., 2008. Thinking outside the zone: high-resolution quantitative diatom biochronology for the Antarctic Neogene. Palaeogeogr. Palaeoclimatol. Palaeoecol. 260, 92–121.
Colleoni, F., De Santis, L., Siddoway, C.S., Bergamasco, A., Golledge, N., Lohmann, G., et al., 2018. Spatio-temporal variability of processes across Antarctic ice-bed-ocean interfaces. Nat. Commun. 9, 2289. https://doi.org/10.1038/s41467-018-04583-0.
Damiani, D., Giorgetti, G., Turbanti, I.M., 2006. Clay mineral fluctuations and surface textural analysis of quartz grains in Pliocene-Quaternary marine sediments from Wilkes Land continental rise (East-Antarctic): paleoenvironmental significance. Mar. Geol. 226, 281–295.
Davey, F.J., 2004. Ross Sea Bathymetry, 1:2000000, Version 1.0. Institute of Geological & Nuclear Sciences geophysical map, 16. Institute of Geological & Nuclear Sciences Limited, Lower Hutt, New Zealand.
DeMaster, D.J., 1981. The supply and accumulation of silica in the marine environment. Geochem. Cosmochim. Acta 45, 1715–1732.
Domack, E.W., 1992. Modern carbon-14 ages and reservoir corrections for the Antarctic Peninsula and Gerlache Strait area. Antarct. J. U. S. 27, 63–64.
Domack, E.W., Harris, P.T., 1998. A new depositional model for ice shelves, based upon sediment cores from the Ross Sea and the Mac. Robertson shelf, Antarctica. Ann. Glaciol. 27, 281–284.
Domack, E.W., Jacobson, E.A., Shipp, S., Anderson, J.B., 1999. Late Pleistocene–Holocene retreat of the West Antarctic ice sheet system in the Ross Sea: part 2. sedimentological and stratigraphic signature. Geol. Soc. Am. Bull. 111, 1517–1536.
Domack, E.W., Jull, A.J.T., Anderson, J.B., Linick, T.W., Williams, C.R., 1989. Application of tandem accelerator mass-spectrometer dating to Late Pleistocene-Holocene sediments of the East Antarctic continental shelf. Quat. Res. 31, 277–287.
Finocchiaro, F., Baroni, C., Colizza, E., Ivaldi, R., 2007. Pre-LGM open-water conditions south of the Drygalski ice tongue, Ross Sea, Antarctica. Antarct. Sci. 19, 373–377.
Finocchiaro, F., Langone, L., Colizza, E., Fontolan, G., Giglio, F., Tuzzi, E., 2005. Record of the early Holocene warming in a laminated sediment core from Cape Hallett Bay (northern Victoria land, Antarctica). Global Planet. Change 45, 193–206.
Folk, R.L., Ward, W.C., 1957. Brazos River bar: a study in the significance of grain size parameters. J. Sediment. Petrol. 27, 3–26.
Friedman, G.M., Sanders, J.E., 1978. Principles of Sedimentology. John Wiley & Sons, New York, p. 139.
Frignani, M., Giglio, F., Langone, L., Ravaioli, M., Mangini, A., 1998. Late Pleistocene-Holocene sedimentary fluxes of organic carbon and biogenic silica in the northwestern Ross Sea, Antarctica. Ann. Glaciol. 27, 697–703.
Grobe, H., Mackensen, A., 1992. Late Quaternary climatic cycles as recorded in sediments from the Antarctic continental margin. In: Kennett, J.P., Warnke, D.A. (Eds.), The Antarctic Paleoenvironment: A Perspective on Global Change. Ant. Res. Ser. 56, 349–376. American Geophysical Union.
Ha, S., Khim, B.K., Colizza, E., Giglio, F., Koo, H.J., Cho, H.G., 2019. Estimation of sediment provenance using clay mineral composition in the Central Basin of the Ross Sea continental margin, Antarctica. Ocean Polar Res. 41, 265–274 (in Korean with English abstract).
Hall, B.L., Henderson, G.M., Baroni, C., Kellogg, T.B., 2010. Constant Holocene southern-ocean ^{14}C reservoir ages and ice-shelf flow rates. Earth Planet Sci. Lett. 296, 115–123.

Khim, B.K., Song, B., Cho, H.G., Williams, T., Escutia, C., 2017. Late Neogene sediment properties in the Wilkes land continental rise (IODP exp. Hole U1359A), East Antarctica. Geosci. J. 21, 21–32.

Ledford-Hoffman, P.A., DeMaster, D.J., Nittrouer, C.A., 1986. Biogenic silica accumulation in the Ross Sea and the importance of Antarctic continental-shelf deposits in marine silica budget. Geochem. Cosmochim. Acta 50, 2099–2110.

Melis, R., Capotondi, L., Torricella, F., Ferretti, P., Geniram, A., Hong, J.K., Kuhn, G., Khim, B.K., Kim, S., Malinverno, E., Yoo, K.C., Colizza, E., 2021. Last Glacial-Holocene paleoenvironmental and climate variability determined from marine microfossils at the Hallett Ridge (northwestern Ross Sea, Antarctica). J. Micropalaeontol. 40, 15–35.

Mezgec, K., Stenni, B., Crosta, X., Masson-Delmotte, V., Baroni, C., Braida, M., Ciardini, V., Colizza, E., Melis, R., Salvatore, M.C., Severi, M., Scarchilli, C., Traversi, R., Udisti, R., Frezzotti, M., 2017. Holocene sea ice variability driven by wind and polynya efficiency in the Ross Sea. Nat. Commun. 8, 1334. https://doi.org/10.1038/s41467-017-01455-x.

Nishimura, A., Nakasone, T., Hiramutsu, C., Tanahashi, M., 1998. Late quaternary paleoenvironment of the Ross Sea continental shelf, Antarctica. Ann. Glaciol. 27, 275–280.

Popp, B.N., Trull, T., Kenig, F., Wakeham, S.G., Rust, T.M., Tilbrook, B., et al., 1999. Controls on carbon isotopic compositions of Southern Ocean phytoplankton. Global Biogeochem. Cycles 13, 827–843.

Quaia, T., Cespuglio, G., 2000. Stable isotope records from the western Ross Sea continental slope (Antarctica): considerations on carbonate preservation. Terra Antartica Rep. 4, 199–210.

Rau, G.H., Sullivan, C.W., Gordon, L.I., 1991. $\delta^{13}C$ and $\delta^{15}N$ variations in Weddell Sea particulate organic matter. Mar. Chem. 35, 355–369.

Reimer, P.J., Bard, E., Bayliss, A., Beck, J.W., Blackwell, P.G., Bronk Ramsey, C., Buck, C. E., Edwards, R.L., Friedrich, M., Grootes, P.M., Guilderson, T.P., Haflidason, H., Hajdas, I., Hatté, C., Heaton, T.J., Hoffmann, D.L., Hogg, A.G., Hughen, K.A., Kaiser, K.F., Kromer, B., Manning, S.W., Niu, M., Reimer, R.W., Richards, D.A., Scott, E.M., Southon, J.R., Turney, C.S.M., van der Plicht, J., 2013. IntCal13 and Marine 13 radiocarbon age calibration curves, 0-50,000 years cal BP. Radiocarbon 55, 1869–1887.

Salvi, C., Busetti, M., Marinoni, L., Brambati, A., 2006. Late quaternary glacial marine to marine sedimentation in the Pennell Trough (Ross Sea, Antarctica). Palaeogeogr. Palaeoclimatol. Palaeoecol. 231, 199–214.

Scherer, R.P., 1994. A new method for the determination of absolute abundance of diatoms and other silt-sized sedimentary particles. J. Paleolimnol. 12, 171–179.

Sjunneskog, C., Scherer, R.P., 2005. Mixed diatom assemblages in glacigenic sediment from the central Ross Sea, Antarctica. Palaeogeogr. Palaeoclimatol. Palaeoecol. 218, 287–300.

Sprenk, D., Weber, M.E., Kuhn, G., Wennrich, V., Hartmann, T., Seelos, K., 2014. Seasonal changes in glacial polynya activity inferred from Weddell Sea varves. Clim. Past 10, 1239–1251.

Taviani, M., Reid, D., Anderson, J.B., 1993. Skeletal and isotopic composition and paleoclimatic significance of Late Pleistocene carbonates, Ross Sea, Antarctica. J. Sediment. Petrol. 63, 84–90.

Tolotti, R., Salvi, C., Salvi, G., Bonci, M.C., 2013. Late Quaternary climate variability as recorded by micropaleontological diatom data and geochemical data in the western Ross Sea, Antarctica. Antarct. Sci. 25, 804–820.

Zielinski, U., Bianchi, C., Gersonde, R., Kunz-Pirrung, M., 2002. Last occurrence datums of the diatoms Rouxia leventerae and Rouxia constricta: indicators for marine isotope stages 6 and 8 in Southern Ocean sediments. Mar. Micropaleontol. 46, 127–137.